Technical Progress Report

for the

DOE/PC/89789--T7

DE92 015801

Third Quarter

(March 1, 1990 - May 31, 1990)

Control of Pyrite Surface Chemistry in Physical Coal Cleaning

by

G.H. Luttrell, R.H. Yoon, J.B. Zachwieja, and M.L. Lagno

Virginia Center for Coal and Minerals Processing
Department of Mining and Minerals Engineering
Virginia Polytechnic Institute and State University
Blacksburg, Virginia 24061-0258

DISCLAIMER

MASTER

ABSTRACT

Correlation of the hydrophobicity measurements of coal and mineral pyrite with changes in the surface composition of the samples as determined by x-ray photoelectron spectroscopy (XPS) reveals that similar surface oxidation products are found on both mineral and coal pyrite samples. The surface oxidation layer of these samples is comprised of different amounts of hydrophilic species (iron hydroxy-oxides and/or iron oxides) and hydrophobic species (polysulfide or elemental sulfur). The resulting hydrophobicity of these samples may be attributed to the ratio of hydrophilic (surface oxides) to hydrophobic (sulfur-containing) species in the surface oxidation layer. Also, coal pyrite samples were found to exhibit a greater degree of superficial oxidation and a less hydrophobic character as compared to the mineral pyrite samples.

INTRODUCTION

The primary objective of this research is to obtain fundamental knowledge concerning the surface properties of coal pyrite as they relate to advanced physical coal cleaning (APCC) processes. This goal will be met by: (1) investigating the mechanisms responsible for the inefficient rejection of coal pyrite and (2) developing schemes for improving the rejection of coal pyrite based on information gathered from part (1).

The goal of this reporting period was to correlate the hydrophobicity measurements with the surface compositional changes as determined by XPS and derive a mechanism or species responsible for the observed changes in hydrophobicity of coal and mineral pyrite.
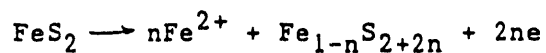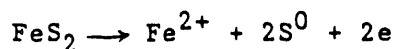
1

EXPERIMENTAL

The data pertaining to hydrophobicity and the corresponding XPS data have been presented in the previous quarterly report. For this reporting period, the XPS data were more closely examined with regard to the mechanism or species responsible for the changes in hydrophobicity of the coal and mineral pyrite samples. Curve resolution of the carbon 2s, oxygen 1s, and sulfur 2p lines was achieved using a curve fitting program with a Gaussian lineshape.

RESULTS and DISCUSSION

The effect of oxidation time in solutions of various pH on mineral and coal pyrite is shown in Figures 1 and 2, respectively. The results clearly show an increase in the amount of surface oxides for both samples with an increase in the oxidation time and pH. Also, these results show that the coal pyrite exhibits a slightly larger percentage of surface oxides. These findings suggest that hydrophilic surface products (ie., iron hydroxy-oxides and/or iron oxides) may be forming and would diminish any natural hydrophobicity exhibited by these samples. In fact, this was the case found and it is best seen in Figures 3 and 4. In Fig. 3, the microflotation recovery of coal and mineral pyrite are plotted as a function of percent surface oxide. The general trend observed is a decrease in the flotation recovery with increasing percentage oxide. Figure 4 represents the induction time of coal and mineral pyrite as a function of percent surface oxide. The trend observed is an increase in induction time with increasing percent oxide which indicates a decrease in hydrophobicity. Moreover, both figures reveal that the hydrophobic character of mineral pyrite is greater than that exhibited by the coal pyrite in the absence of any flotation surfactants.

Tables 1 and 2 provide a summary of the sulfur 2p data obtained for the mineral and coal pyrite samples, respectively. The sulfur 2p spectra could not be fitted with a single doublet having the position and size corresponding to published spectra for pyritic sulfur. An additional doublet of lesser intensity at a higher binding energy had to be included in order to obtain an acceptable fit. These results indicate that, in addition to the lattice sulfide, the surface contains altered sulfur species produced by superficial oxidation. These non-sulfide species were observed in both the mineral and coal pyrite samples and occured over the entire pH range. The positon of these non-sulfide species was found to be quite similar to that observed for either a polysulfide or elemental sulfur. The presence of either of these species on the surface is believed to impart hydrophobicity to the sample. Possible oxidation mechanisms of the pyrite samples in acidic and basic environments may be described as follows:

Acidic:

$$FeS_2 \longrightarrow Fe^{2+} + 2S^0 + 2e$$

$$FeS_2 \longrightarrow nFe^{2+} + Fe_{1-n}S_{2+2n} + 2ne$$

Basic:

$$FeS_2 + 3nOH^- \longrightarrow nFeOOH + Fe_{1-n}S_{2+2n} + nH_2O + 3ne$$

Figures 5 and 6 show the result of microflotation recovery and induction time of mineral and coal pyrite in the absence of flotation surfactants plotted as a function of percent polysulfide or elemental sulfur (non-sulfide species). Again, similar to Figs. 3 and 4, the hydrophobic character of the mineral pyrite sample is greater than the coal pyrite sample and the data for the two samples cannot be normalized to one curve. These findings suggest that the observed hydrophobicity of the samples may be the result of competing hydrophilic and hydrophobic surface sites.

Since either the percentage surface oxide or the percent polysulfide or elemental sulfur alone cannot adequately describe the observed differences in hydrophobicity between the mineral and coal pyrite samples, the combination of the two was considered. In Figures 7 and 8 the ratio of the oxygen-1s to sulfur-2p peak intensity is plotted for mineral and coal pyrite, respectively. This ratio provides a measure of the extent to which the surface is superficially oxidized. In both cases, the surfaces of the pyrite samples become more oxidized with increasing pH and conditioning time. However, the data indicate that the initial degree of oxidation of the coal pyrite sample is significantly higher than that for the mineral pyrite, which was not that obvious when considering only the percentage of surface oxide (Figs. 1 and 2). This difference in oxidation appears to be maintained across the entire pH range and may provide an explanation for the comparatively weaker floatability of the coal pyrite sample.

In order to examine the effects of the surface oxidation on the nature of the mineral and coal pyrite surfaces, the hydrophobicity results were plotted as a function of the ratio of the oxygen-1s to sulfur-2p peak intensity. These plots are shown in Figures 9 and 10 for the microflotation recovery and induction time, respectively. As shown, there is a steady decrease in floatability and increase in induction time as the surface of the pyrite samples become more oxidized. Moreover, the hydrophobicity data for the two different samples can be normalized to the same curve. Thus, the differences observed between the hydrophobicity of the mineral and coal pyrite appear to be attributable to differences in oxidation.

Since the coal pyrite samples exhibit a greater degree of superficial oxidation, they are less hydrophobic and can be more easily rejected during flotation. Unfortunately, the presence of flotation surfactants, such as frothers and collectors have been shown to improve the floatability of weakly

4

hydrophobic mineral and coal pyrite (see the previous quarterly report).

CONCLUSIONS and FUTURE WORK

The results presented in this report clearly indicate that the observed hydrophobicity of mineral and coal pyrite samples may be attributed to the ratio of hydrophilic (surface oxides) to hydrophobic (polysulfide or elemental sulfur) species in the surface oxidation layer. However, the mechanism responsible for the production of the hydrophobic surface species is not fully understood at this time. Therefore, future studies will be directed toward elucidating this mechanism. The studies will include electrochemistry coupled with spectroscopic techniques (XPS and infrared reflectance). Synthesis and characterization of polysulfide compounds will be performed to corroborate the XPS results. Moreover, in-situ Raman spectroscopy will be conducted on both mineral and coal pyrite samples to determine the composition and structure of the surface oxidation layer .

Table 1.   Curve-resolved XPS peak positions of the sulfur 2p line for mineral pyrite as a function of pH and oxidation time.

MINERAL PYRITE
Huanzala, Peru

| Oxidation Time (min) | pH | S2p 3/2 | | Percent Sulfide |
		Sulfide (ev)	Non-Sulfide (ev)	
20	4.6	162.2	164.0	86
90	4.6	162.5	164.4	88
300	4.6	162.5	164.6	89
20	6.8	162.5	164.1	86
90	6.8	162.5	164.1	86
300	6.8	162.6	164.3	85
20	9.2	162.3	163.9	91
300	9.2	162.3	163.9	91
1 mth	9.2	---	---	--
Dry Grind		162.1	163.4	80

Table 2. Curve-resolved XPS peak positions of the sulfur 2p line for coal pyrite as a function of pH and oxidation time.

COAL PYRITE
Pocahontas No. 3 Seam

Oxidation Time (min)	pH	S2p 3/2 Sulfide (ev)	Non-Sulfide (ev)	Percent Sulfide
20	4.6	161.9	163.5	84
90	4.6	161.9	163.6	84
300	4.6	161.9	163.9	90
20	6.8	162.2	163.8	90
90	6.8	162.2	164.0	89
300	6.8	162.3	163.9	89
20	9.2	162.0	163.6	86
90	9.2	162.2	163.9	95
300	9.2	162.1	163.8	96
Dry Grind		162.3	164.2	87
Air Oxidized		162.5	164.8/167.9	82
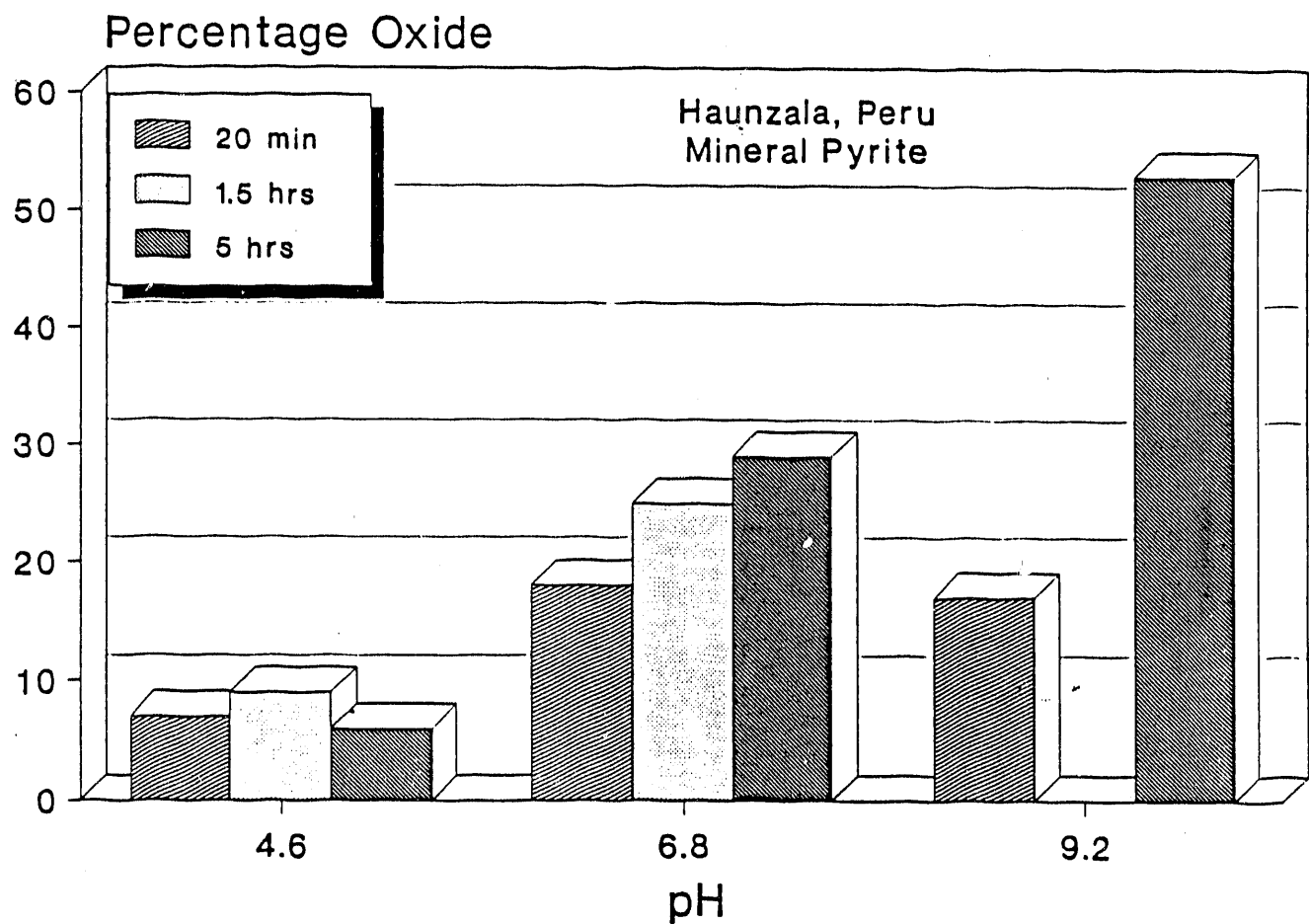
Figure 1. The effect of pH and oxidation time on the percentage oxide determined by XPS for mineral pyrite.
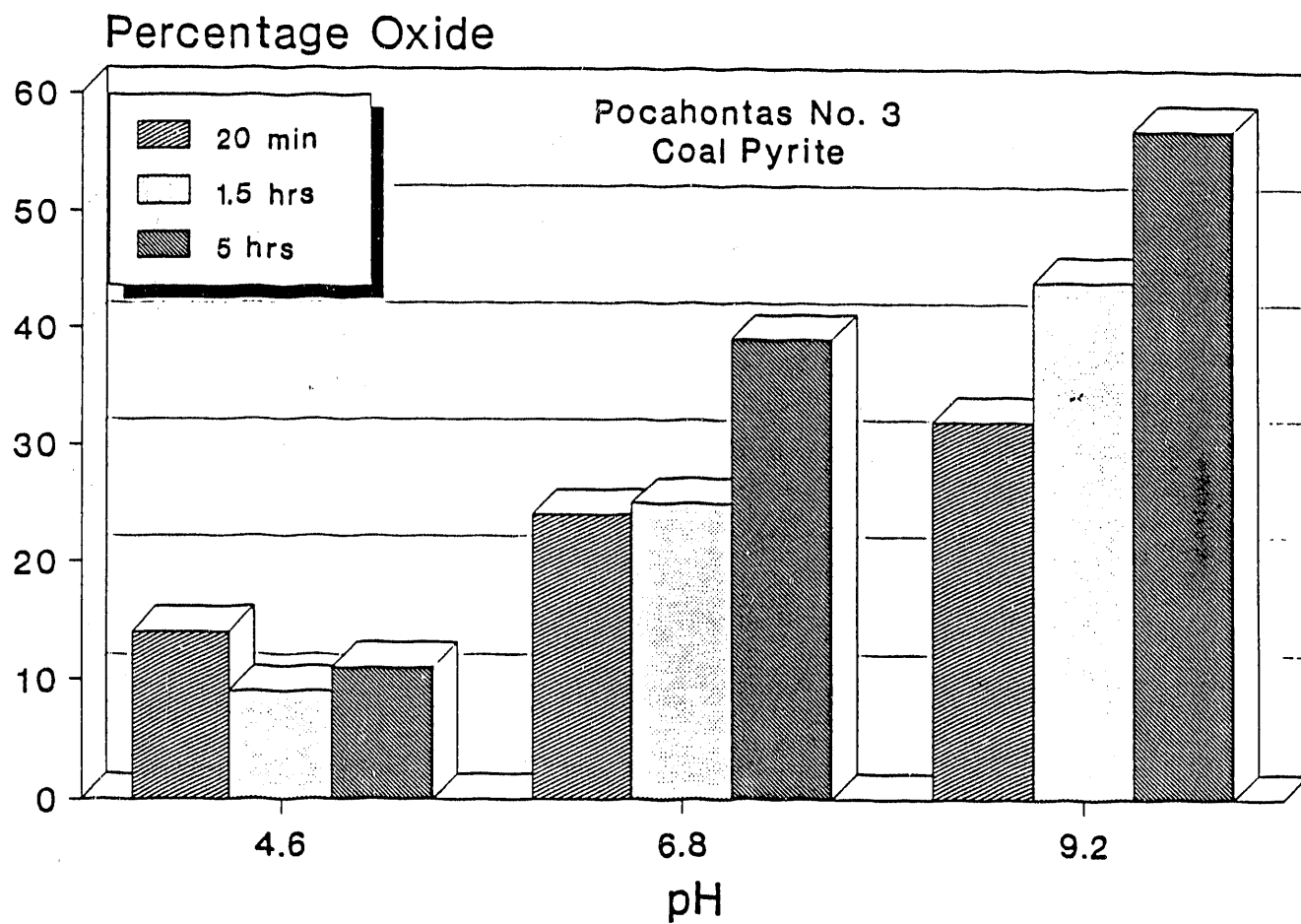
Figure 2. The effect of pH and oxidation time on the percentage oxide
determined by XPS for coal pyrite.
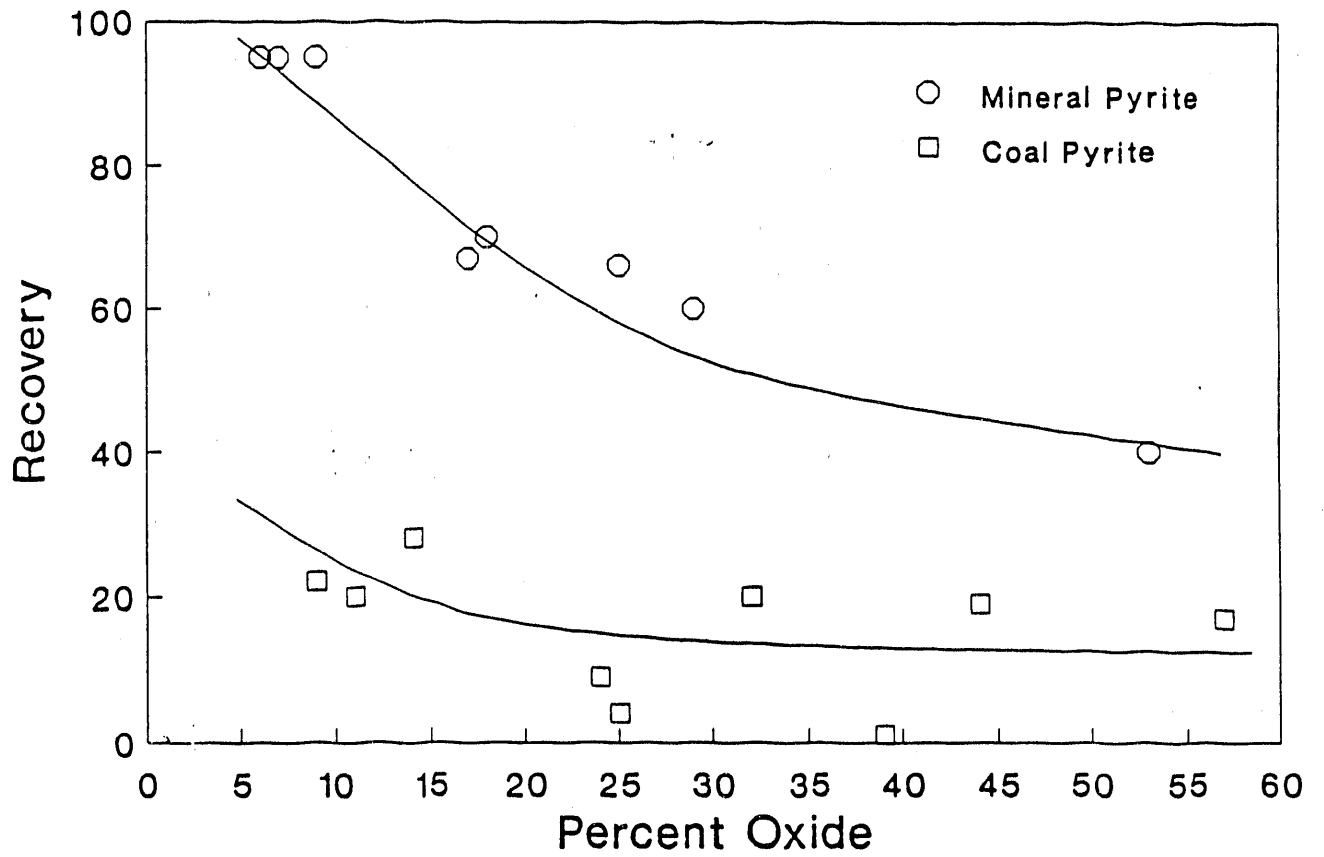
Figure 3. The relationship between microflotation recovery and the percent oxide for mineral and coal pyrite samples.
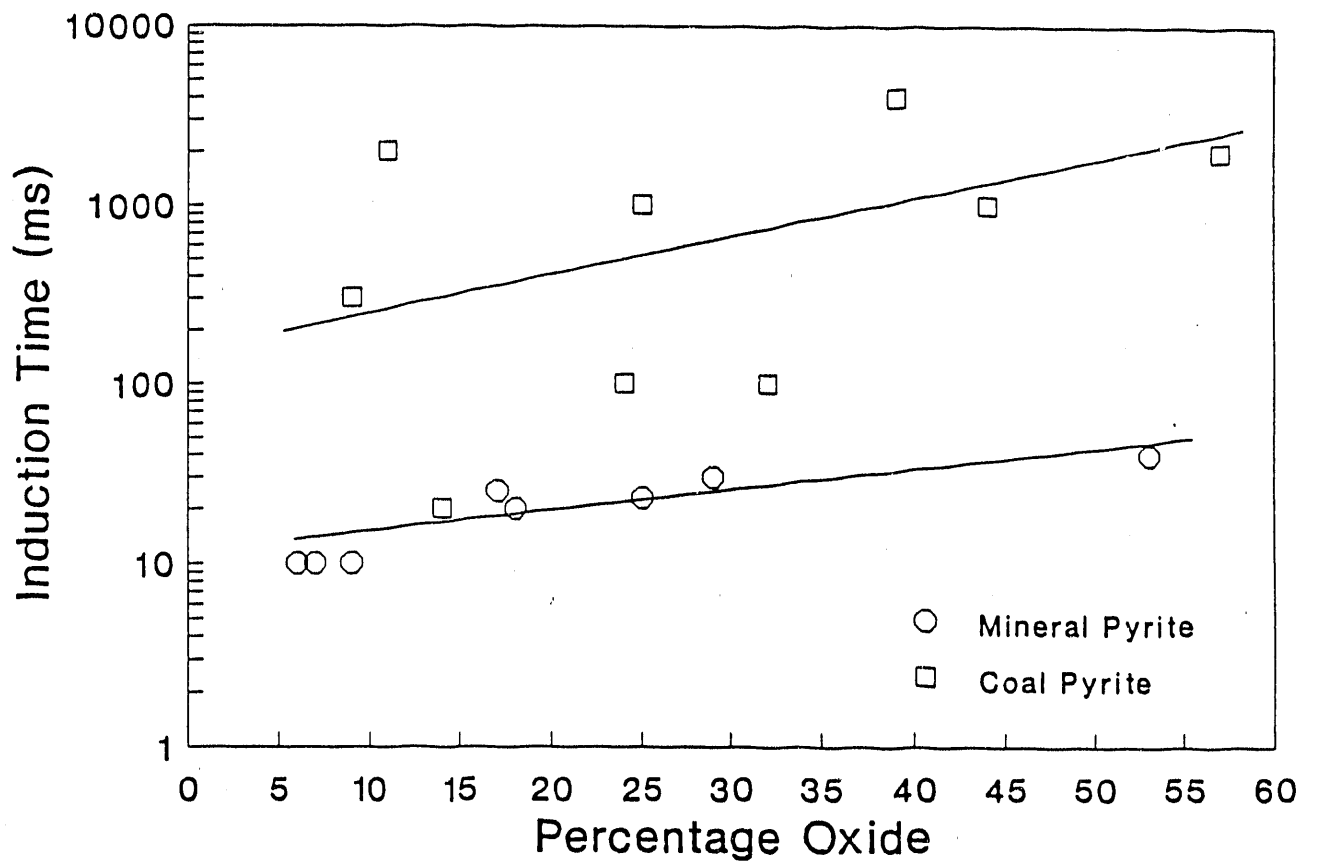
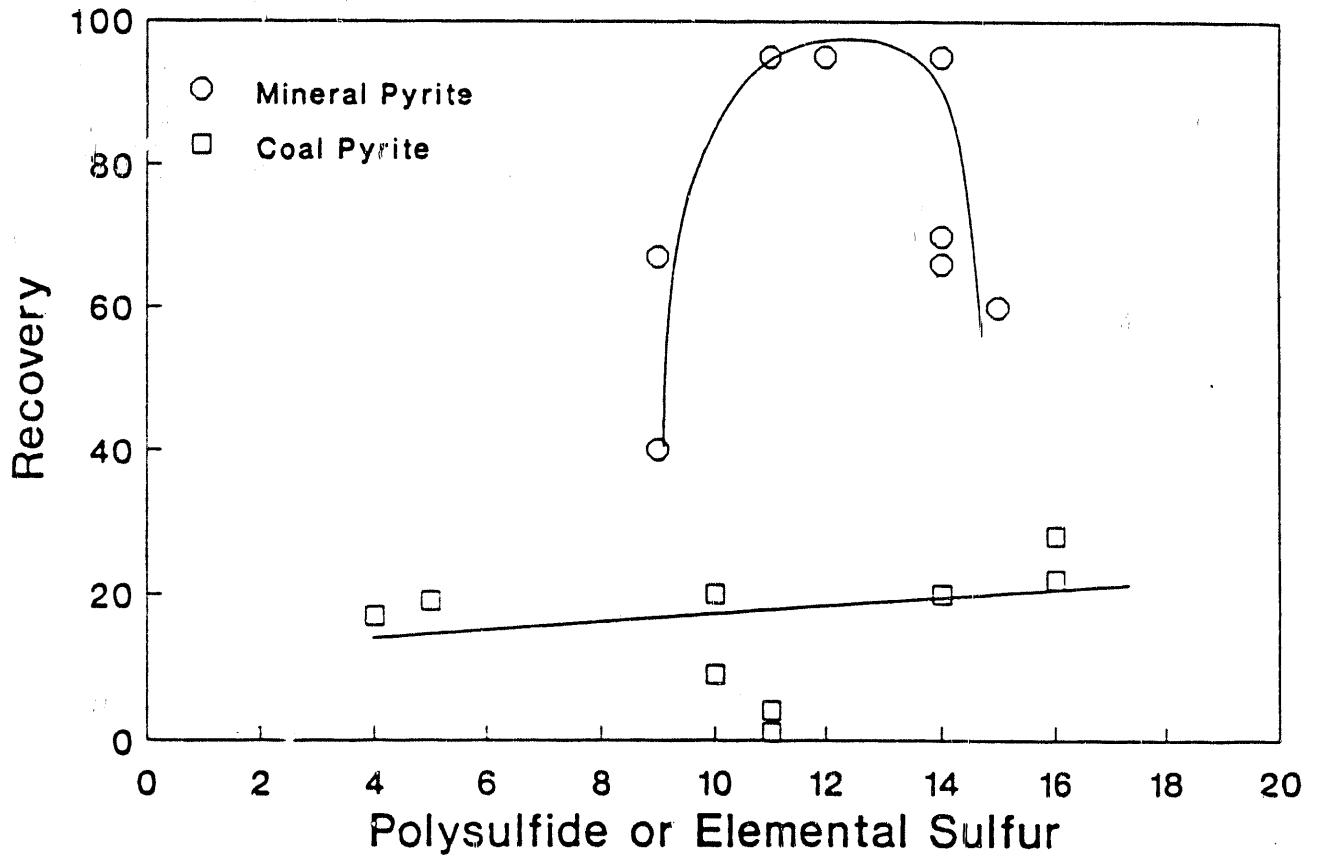Figure 4. The relationship between induction time and the percent oxide for mineral and coal pyrite samples.

Figure 5. The relationship between microflotation recovery and the percent polysulfide or elemental sulfur for mineral and coal pyrite samples.
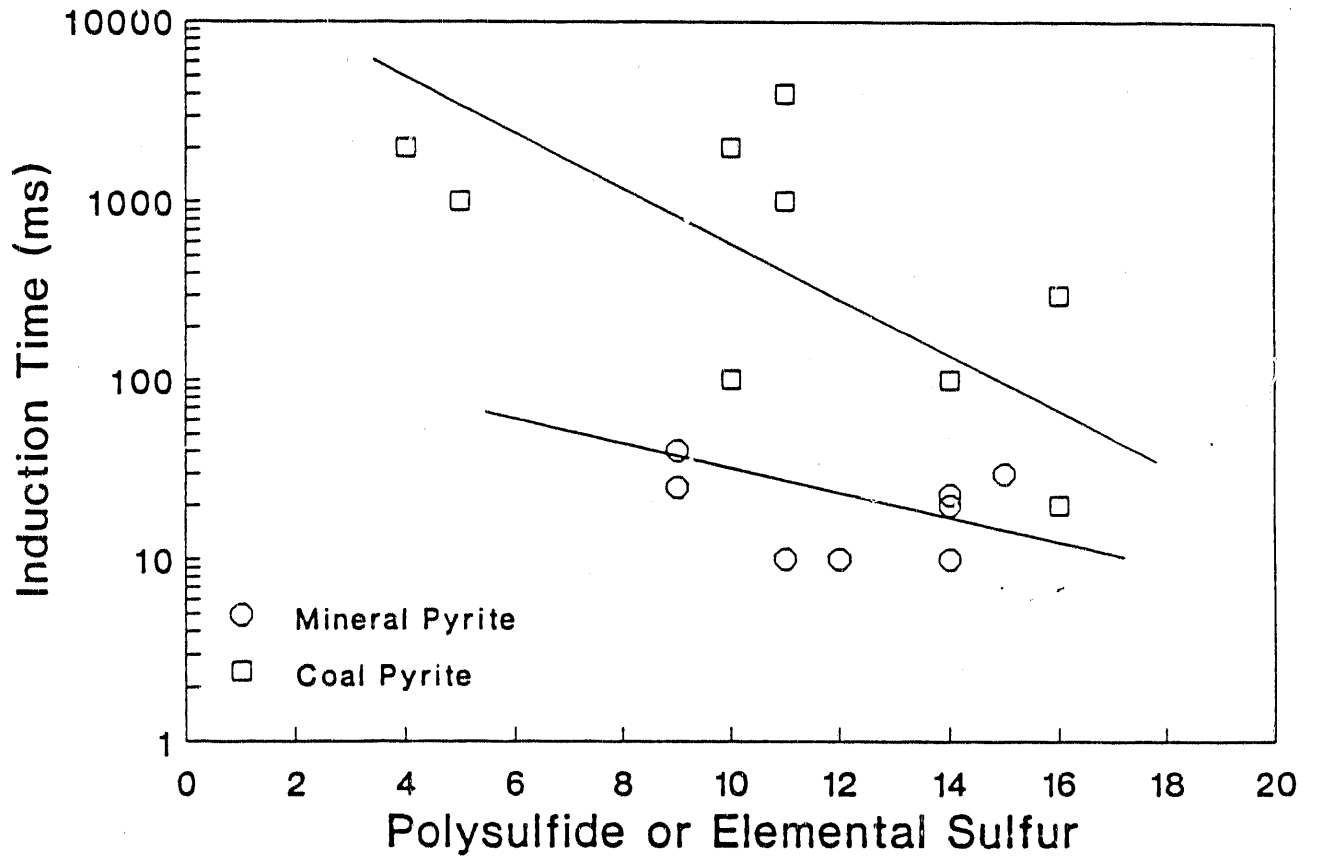
Figure 6. The relationship between induction time and the percent polysulfide or elemental sulfur for mineral and coal pyrite samples.
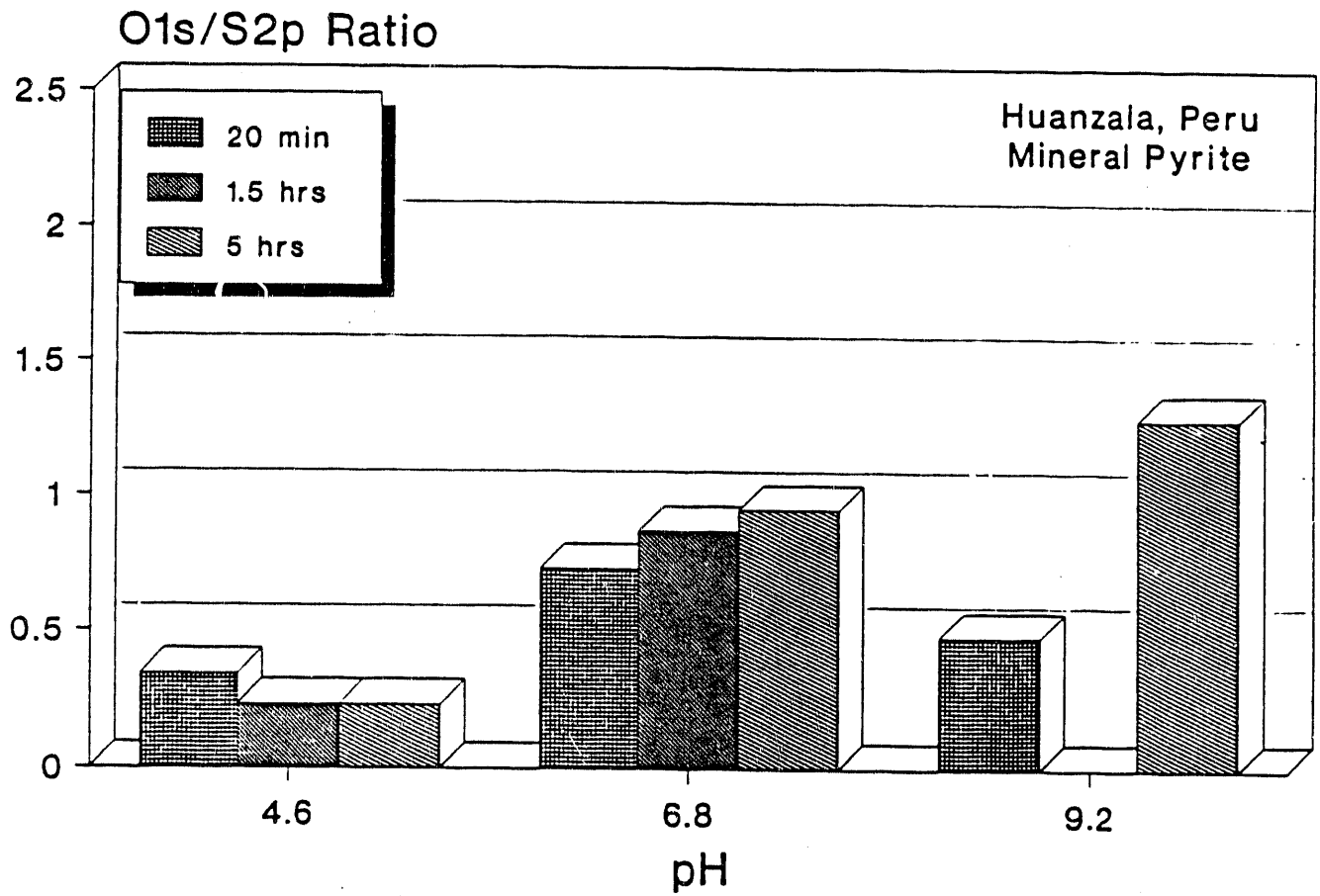
O1s/S2p Ratio

Figure 7. The effect of pH and oxidation time on the oxygen-1s to sulfur-2p surface ratio determined by XPS for mineral pyrite.
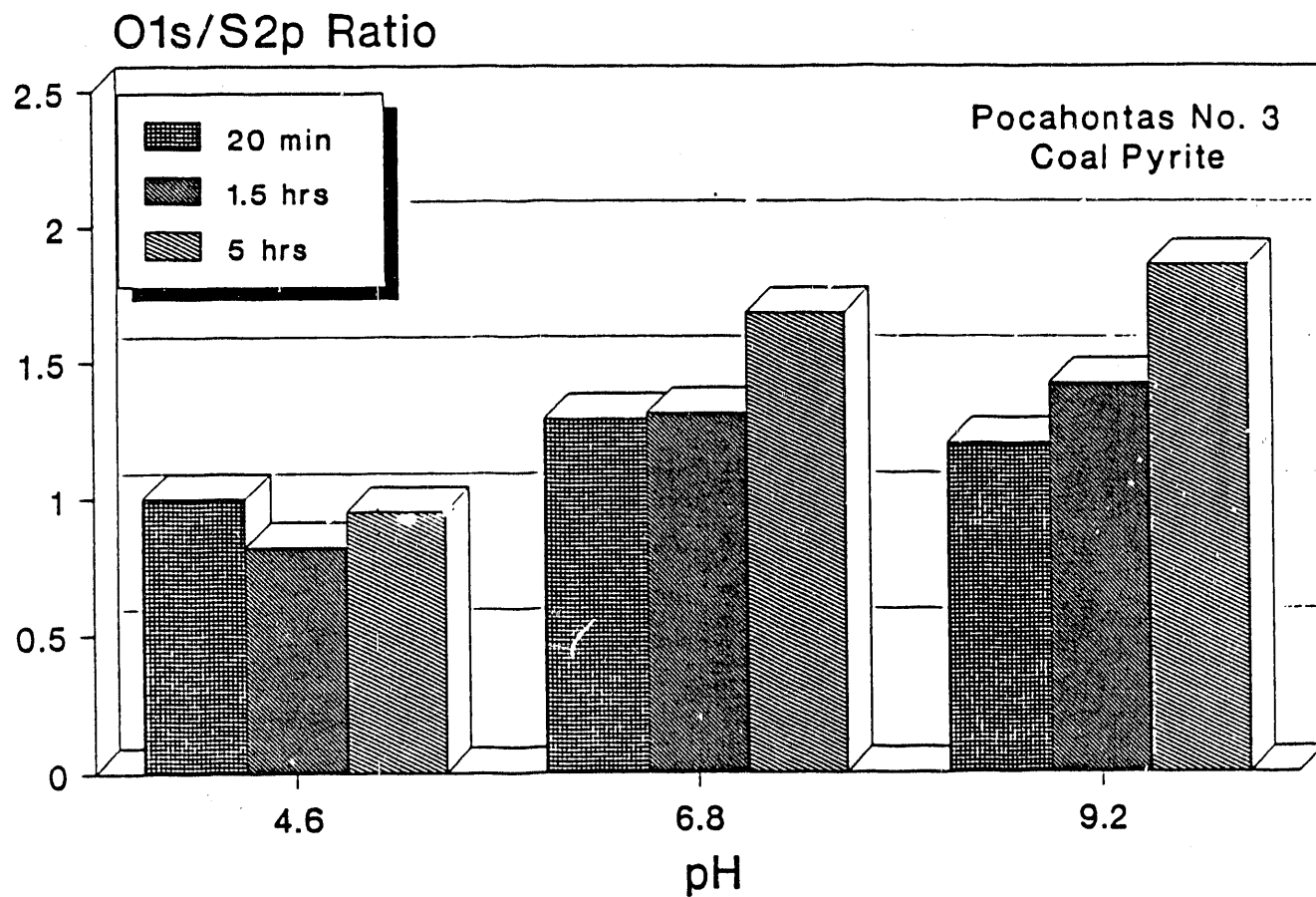
Figure 8. The effect of pH and oxidation time on the oxygen-1s to sulfur-2p surface ratio determined by XPS for coal pyrite.
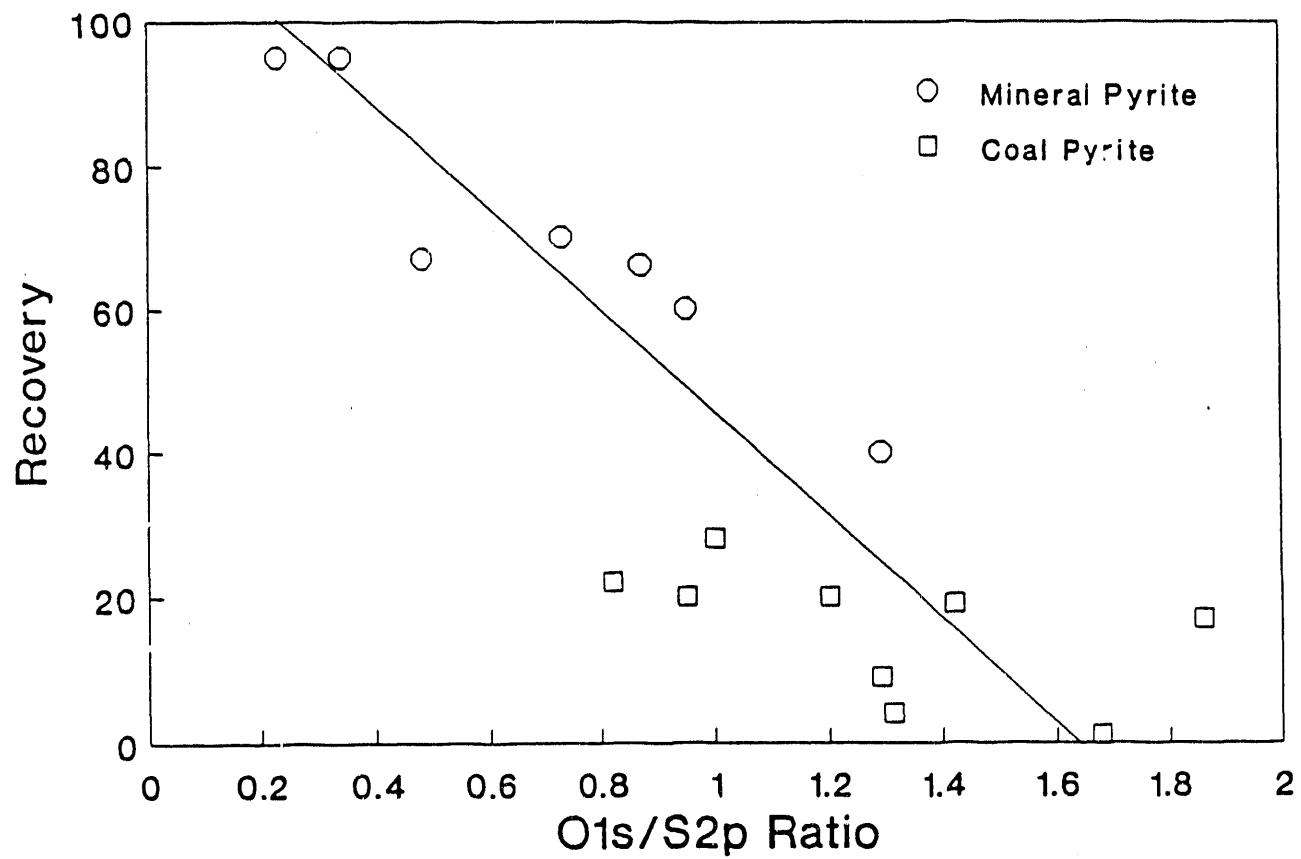
Figure 9. The relationship between microflotation recovery and the oxygen-1s to sulfur-2p ratio for mineral and coal pyrite samples.
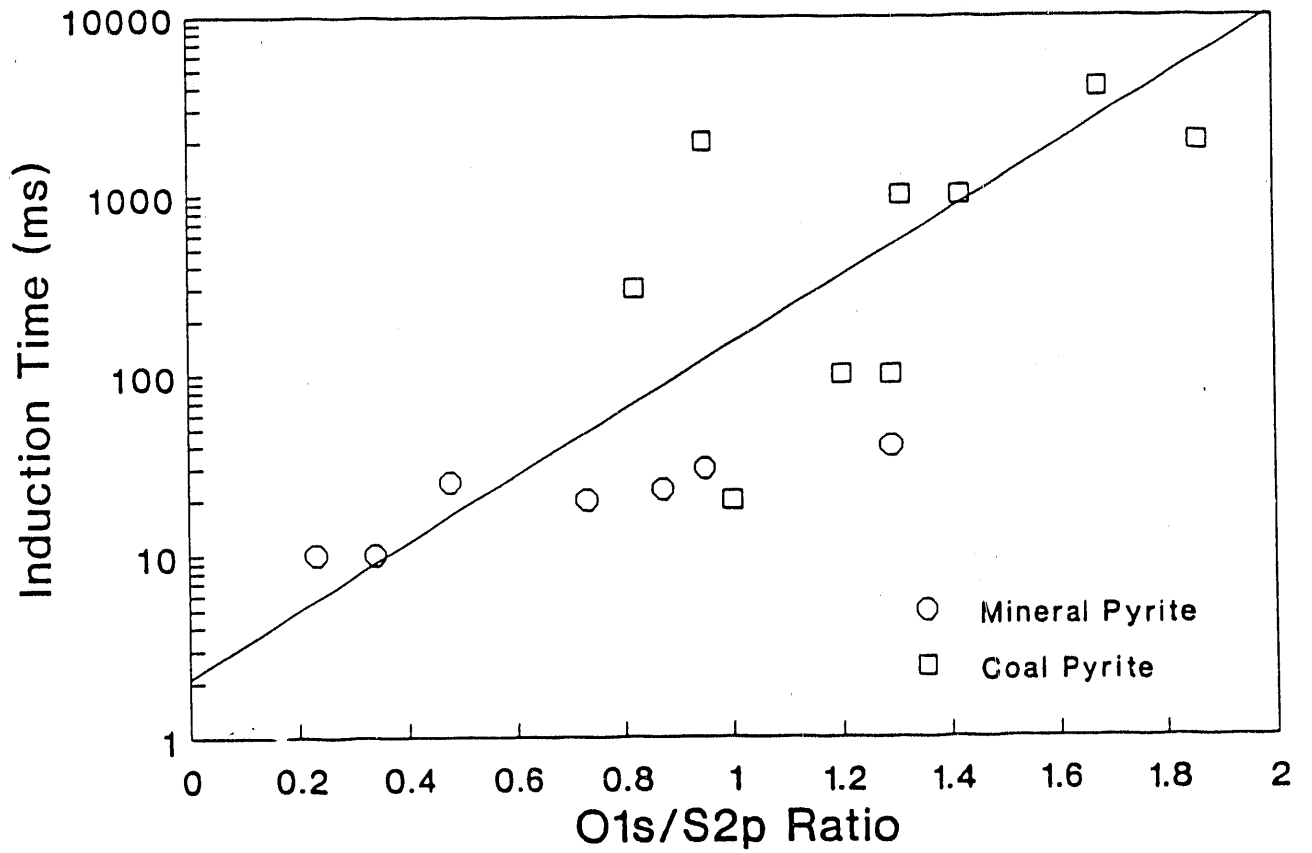
Figure 10. The relationship between induction time and the oxygen-1s to
sulfur-2p ratio for mineral and coal pyrite samples.

END

DATE
FILMED
8 / 11 / 92